ARCHIVES
of
FOUNDRY ENGINEERING

ISSN (2299-2944)
Volume 2025
Issue 4/2025

162 – 166

21/4

10.24425/afe.2025.157614

Published quarterly as the organ of the Foundry Commission of the Polish Academy of Sciences

Effect of the Directional Crystallization Obtained by the Bridgman Method on the Thermoelectric Properties of Bi_2Te_3

K. Bracka-Kęsek *, B. Rafałowski, D. Kopyciński
AGH University of Krakow, Poland
* Correspondence contact: e-mail: bracka@agh.edu.pl

Received 15.07.25; accepted in revised form 30.10.25; available online 31.12.2025

Abstract

Bi_2Te_3-based alloys are widely employed in the fabrication of thermoelectric modules for low- and medium-temperature applications. This paper investigates a novel approach to the production of structure-oriented thermoelectric materials, comparing the results with those obtained from polycrystalline materials synthesized via powder metallurgy. The strength properties of thermoelectric materials produced from metal powders are much lower than those produced by directional crystallization methods. As anticipated, samples exhibiting an oriented structure, approaching monocrystalline properties, demonstrated superior performance. Furthermore, directional crystallization technology in a Bridgman furnace was investigated, using the LMC (liquid metal cooling) method, which facilitates the achievement of the desired alloy microstructure. The most favorable results were achieved in a sample produced through directional crystallization in a Bridgman apparatus specifically designed for this research. While all fabricated samples exhibited comparable performance, a sample possessing an oriented crystal structure exhibited the highest ZT parameter of 0.5 at a temperature of 520K. This research highlights the potential of structure-oriented thermoelectric materials for enhanced performance in thermoelectric devices.

Keywords: Bi_2Te_3, Single crystal, Bridgman method, Thermoelectric properties, LMC - Liquid Metal Cooling

1. Introduction

Thermoelectric materials are gaining significant traction due to their diverse applications, particularly in areas where conventional alternatives are either impractical or highly undesirable. These materials, capable of converting thermal energy into electrical energy and vice versa, find utility in a wide range of fields, including refrigeration, energy harvesting, military devices, telecommunications equipment, electronics, optoelectronics, and temperature control and monitoring [1,2]. In metal foundries, it is possible to use the heat released during the crystallization process in a useful way. In the era of energy transformation, one of the postulates of sustainable development is to increase energy efficiency in heavy industry. In foundries, this postulate can be implemented using waste heat generated during the foundry process [3]. Thermoelectric generators are devices that directly convert heat into electricity, and can be used wherever waste heat can be harvested to increase Energy efficiency and, as a consequence, reduce the consumption of energy from other sources. The thermoelectric figure of merit, ZT, quantifies the efficiency of thermal energy conversion, serving as a crucial indicator of material quality. A greater dimensionless figure of merit ZT corresponds to superior thermoelectric properties. The ZT coefficient is intricately linked to thermal conductivity (λ) and electrical conductivity (σ), as defined by the equation:

$$ZT = \frac{\alpha^2 \cdot \sigma}{\lambda} \cdot T$$

where α represents the Seebeck coefficient. This interdependence poses a significant challenge, as these properties are often influenced by the same underlying physical phenomena. Bismuth telluride (Bi_2Te_3) stands out as one of the most promising thermoelectric materials. Belonging to the A_2B_3 chalcogenide family (A = Bi/Sb, B = Te/Se), it crystallizes in the rhombohedral system with the space group R3m. The material comprises hexagonal Bi and Te planes, arranged in a five-layer unit cell with an atomic sequence of Te-Bi-Te-Bi-Te. This arrangement forms a rhombohedral lattice with three five-layer units per unit cell. These units are stacked vertically with weak van der Waals forces between them, facilitating cleavage. Despite their potential, the synthesis of these materials is often complex and time-consuming [4-6]. Conventional methods include rapid crystallization from the melt or powder metallurgy techniques. The vertical Bridgman method offers a promising approach for growing large, high-quality single crystals. While several studies have explored the challenges associated with single crystal growth of Bi_2Te_3 using the Bridgman technique, a comprehensive and systematic investigation remains lacking [7-9].

2. Experiment

The synthesis of materials was carried out in graphite-coated quartz ampoules evacuated to a residual pressure of 10−5 mbar. Polycrystalline $Bi_2Te_{3-x-y}Se_xCl_y$ (x = 0.6, y = 0.015; x = 0.6, y = 0.03; x = 0.3, y = 0.015; x = 0.3, y = 0.03; and x = 0.6, y = 0) specimens were synthesized by melting the elements Bi (Alfa Aesar, 99.999%), Te (Alfa Aesar, 99.999%), Se (Alfa Aesar, 99.999%), and $BiCl_3$ (Alfa Aesar, 99.999%)) at 1123 K in a rocking furnace and then quenched in cold water. The resultant ingots were crushed into fine powders by ball milling and densified by the spark plasma sintering (SPS) technique at 673 K for 10 min in a 12.7 mm diameter graphite mold under an axial compressive stress of 45 MPa in an argon atmosphere. The heating/cooling rate was 50 K/min.

The crystallization of Bi_2Te_3 was conducted employing the vertical Bridgman technique within a custom-designed apparatus developed for the AGH Foundry Department (Fig. 1). The key part of the apparatus is the construction of a cooler (Fig. 2) operating on the principle of the LMC technique [10]. A quartz ampoule, measuring approximately 160 mm in length with an external diameter of 7 mm and a wall thickness of 2 mm, was utilized. A sharp tip was incorporated at the ampoule's terminus to induce single nucleation, facilitating the growth of a well-defined single crystal. Following preparation, the ampoule underwent thorough cleaning with double-distilled water, followed by rinsing with acetone and methanol, and subsequent drying for 5 hours in a heated oven. Subsequently, 19 g of commercially available Bi_2Te_3 material, exhibiting a purity of 99.98% (manufacturer: Alfa Aesar), was carefully introduced into the ampoule. This material quantity occupied approximately 50 mm of height within the prepared ampoule. The filled ampoule was then subjected to a dynamic vacuum of ~10^{-5} mbar and meticulously sealed. The ampoule was subsequently suspended within a single-zone resistance furnace, positioning the tip 580 mm from the furnace's top. Temperature control was maintained using a Eurotherm temperature controller (model no: 2404) with a precision of ±10°C. The furnace temperature was then elevated to ≈620°C, exceeding the melting point (≈585-587°C) of Bi_2Te_3, and held at this temperature for 12 hours to ensure complete homogenization. Crystallization was initiated by carefully moving the ampoule downward through the furnace at a controlled rate of ≈ 7 mm/h, followed by gradual cooling at varying rates until reaching ambient temperature. The crystallization process yielded a cylindrical sample, approximately 4 cm in height, conforming to the shape of the quartz ampoule.

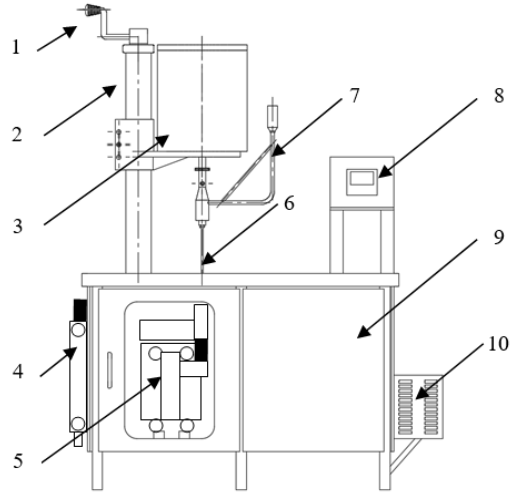

Fig. 1. Schematic of the furnace for directional crystallization, using the Bridgman-Stockbarger method with the LMC technique. The numbers indicate: 1 - Screw gear, 2 - Guide column, 3 - Furnace, 4 - Water cooling system, 5 - Drive and gear assembly, 6 - Pull rod, 7 - Batch cooler, 8 - HMI panel, 9 - PLC, 10 - Power transformer

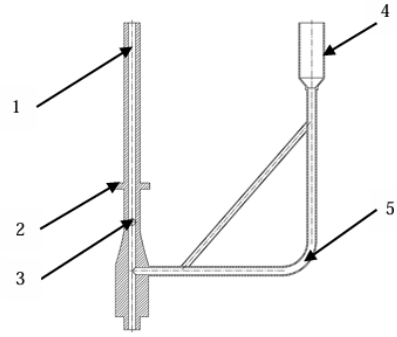

Fig. 2. Schematic of the Batch cooler enabling the use of the LMC technique for Bridgman-Stockbarger directional crystallization. The numbers indicate:1 - Head with a hole for the pull rod, 2 - Attaching the head with a knob to the furnace body, 3 - Cooling water inlet/outlet (from the mains) on one and the opposite side of the head, respectively, 4 - Tank for the cooling medium, 5 - Circulation of the cooling medium

Table 1.
Summary of thermoelectric parameters for selected preparation methods

Method	Parameter									
	Electrical conductivity [S]		Seebeck coefficient [μv/K]		Power factor [μW/cmK^2]		Thermal conductivity [W/mK]		Thermoelectric figure of merit ZT [W/mK]	
	Min.	Max.	Min.	Max.	Min.	Max.	Min.	Max.	Min.	Max.
Directional without cooling LMC	1000	2500	-125	-105	13	27	2,5	3,3	0,25	0,5
Directional with cooling LMC	1250	2700	-104	-50	10	13	2,1	3,8	0,07	0,42
Powder (SPS)	1000	2750	-122	-87	11	13	1,8	2,5	0,14	0,47

3. Results

After making two single crystal tests in an experimental piece for Bridgman crystallization, metallographic tests and thermoelectric tests were performed on them. The samples were cut according to the scheme (Fig. 3) and the flow, which is intended for a specific type of test.

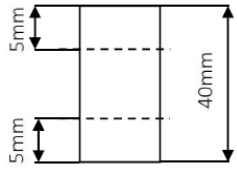

Fig. 3. Schematic of cutting samples for measurements

3.1 Thermoelectric properties

The experimental results, while generally consistent with the authors predictions, exhibit slight deviations from parameters reported in previous studies. This suggests that the crystallization process may not have been fully optimized, necessitating adjustments to the selected parameters for future enhancements in material properties. Furthermore, the SPS-synthesized samples also displayed suboptimal performance compared to literature values, indicating potential shortcomings in their fabrication process. Despite these variations, the presented thermoelectric data (Table 1, Fig. 6 and Fig.7) demonstrate a degree of consistency, highlighting the appropriate selection of the production technology. Notably, the Bridgman technique yielded the most favorable results, justifying its continued use. The SPS method achieved the highest electrical conductivity (σ = 2750 S), while Crystal 1 exhibited the lowest Seebeck coefficient (α = -125 μV/K). Crystal I, fabricated without LMC cooling, attained the highest power factor (PF = 27 μW*cm^{-1}K^{-2}). The Bridgman technique, also without LMC cooling, yielded the lowest thermal conductivity (λ = 1.8 W/mK). While the ZT parameter exhibited comparable values across all samples, Crystal 1 displayed the highest coefficient (ZT = 0.5). A comparative analysis of electrical conductivity reveals a notable increase of approximately 200 S in Crystal 2 compared to Crystal 1, approaching the maximum value of 2750 S achieved by the SPS method.

3.2 Structural properties

Prior to microscopic and macroscopic analysis, the samples underwent meticulous preparation. The initial stage involved precise cutting according to a predetermined scheme (Fig. 2) followed by mounting. Subsequently, the samples were meticulously prepared in accordance with material specifications using a dedicated polishing and grinding machine (Fig. 3), supplemented by manual grinding on sandpaper with diamond suspension and polishing paste. The thus-prepared samples were then subjected to examination under a metallographic microscope. The accompanying figures 4 and 5 depict their longitudinal (a) and cross-sectional (b) views, illustrating the macrostructure of the material.

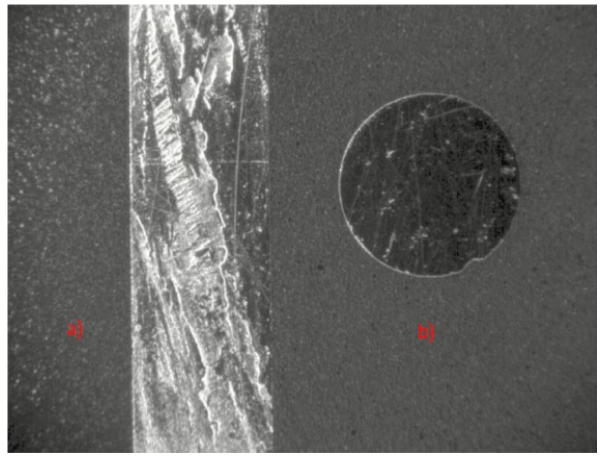

Fig.4. Macrostructure of the Crystal 1, longitudinal view of the sample (a) and cross-sectional view of the sample (b)

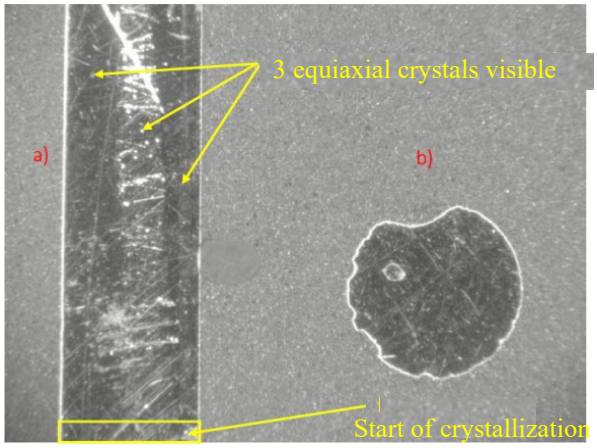

Fig.5. Macrostructure of the Crystal 2, longitudinal view of the sample (a) and cross-sectional view of the sample (b)

To compare the test results, the values obtained from thermoelectric tests for each of the methods of preparation were used and presented in the table (Table 1). However, it was not possible to compare the results of metallographic tests, due to the lack of microscopic photos of the crystals. And these could not be taken because their surface turned out to be degraded after too intensive etching with sulfuric acid H_2SO_4, therefore, instead of the microstructure, photos of the macrostructure of the samples were taken. Fig.6 presents Seeback effect maps for the obtained crystals in longitudinal and transverse sections. The parameter and maps differ significantly for the two crystals. Different scales are presented for the results. Crystal 1 achieved values in the range of -250 to -100, while Crystal 2 -100 to 0.

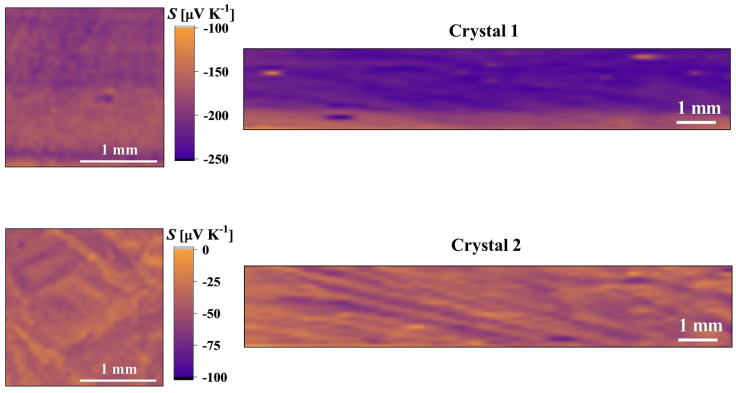

Fig.6. Spatial distribution of the Seebeck coefficient on the polished surface

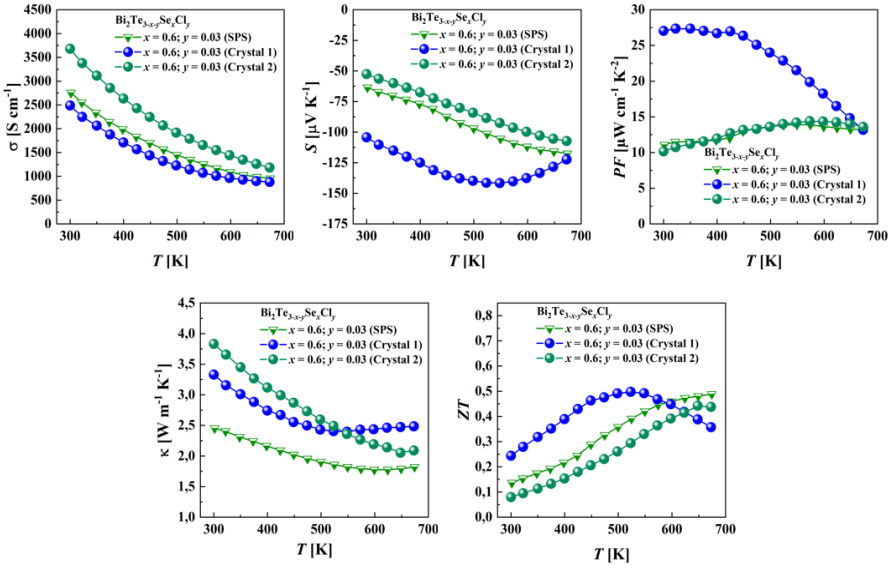

Fig. 7. The graphs show, in order, the measurements of Electrical Conductivity, Seebeck Coefficient, Power factor, Thermal Conductivity, Thermoelectric figure of merit ZT

4. Conclusion

The experimental results strongly support the validity of the chosen crystallization parameters. However, the etching and structural analysis methodologies require refinement, and the efficiency of the directional crystallization process should be further optimized. Notably, the temperature gradient (G) at the crystallization front should be precisely defined to ensure consistency with current specialist literature on the materials employed in this study. Reducing the crystallization speed (S_k), specifically by decreasing the pull rod withdrawal rate from the cooler cylinder, is anticipated to achieve this effect. Additionally, exploring variations in the temperature gradient (G) could prove beneficial. As evident from Table 1 and and Fig. 7, thermoelectric parameters obtained using powder metallurgy methods also exhibit deviations from ideal values (ZT = 0.14 - 0.47). Therefore, the utilization of directional crystallization methods is justified, particularly considering the achieved ZT values of 0.25 - 0.5. It is crucial to emphasize that directional methods represent a more effective approach to producing thermoelectric materials, albeit requiring specialized knowledge to attain the highest market-available quality. Such high-performance materials encompass compounds with highly sophisticated crystal structures, including SKD, PLEC, TAGS, and PGECThe thermoelectric parameters of the materials obtained are shown as a function of temperature. Thus, the operating temperature of a given thermoelectric material will be crucial for the efficiency of electricity recovery. Moreover, the high ZT parameter was obtained at different temperatures, thus opening the potential to use the developed n-type Bi2Te3-based materials for the fabrication of the functionally graded thermoelectric leg.

Acknowledgements

The authors would like to thank WIMIC faculty AGH in Kraków members, especially prof. dr. Krzysztof Wojciechowski and dr. Taras Parashchuk, for their assistance with the thermoelectric study.

References

[1] Bell, L.E. (2008). Cooling, heating, generating power, and recovering waste heat with thermoelectric systems. *Science*. 321(5895), 1457-1461. https://doi.org/10.1126/science.1158899.

[2] Królicka, A., Hruban, A. & Mirowska, A. (2012). Modern thermoelectric materials - literature review. *Materiały Elektroniczne*. 40, 19-34. (in Polish).

[3] Paczkowski, P., Wojciechowski, W., Kopyciński, D. (2024). Control of casting structure and production of electricity by means of a chill with thermoelectric modules. In ICT/ECT 2024: 40th International and 20th European Conference on Thermoelectrics, 30-June – 4 July 2024 (pp. 440). Krakow, Poland.

[4] Parashchuk, T., Knura, R., Cherniushok, O. & Wojciechowski, K. (2022). Ultralow lattice thermal conductivity and improved thermoelectric performance in Cl-doped Bi2Te3–xSex alloys. *ACS Applied Materials & Interfaces.* 14(29), 33567-33579. https://doi.org/10.1021/acsami.2c08686.

[5] Knura, R., Maksymuk, M., Parashchuk, T. & Wojciechowski, K. (2024). Achieving high thermoelectric conversion efficiency in based stepwise legs through bandgap tuning and chemical potential engineering. *Dalton Transactions*. 53, 123-135.

[6] Cherniushok, O., Parashchuk, T., Snyder, J. & Wojciechowski, K. (2025). Discovery of a new Cu-based chalcogenide with high near room temperature: low-cost alternative for the based thermoelectric. *Advanced Materials*. 37(18), 2420556, 1-12. https://doi.org/10.1002/adma.202420556.

[7] Keawprak, N., Lao-Ubol, S., Eamchotchawalit, C. & Sun, Z.M. (2011). Thermoelectric properties of Bi2SexTe3− x prepared by Bridgman method. *Journal of Alloys and Compounds*. 509(38), 9296-9301. https://doi.org/10.1016/j.jallcom.2011.06.116.

[8] Krishna, A., Vijayan, N., Singh, B., Thukral, K. & Maurya, K.K. (2016). Crystalline perfection and mechanical investigations on vertical Bridgman grown Bismuth telluride (Bi_2Te_3) single crystals for thermoelectric applications. *Materials Science and Engineering: A*. 657, 33-37. https://doi.org/10.1016/j.msea.2016.01.033.

[9] Kuznetsov, V.L., Kuznetsova, L.A., Kaliazin, A.E. & Rowe, D.M. (2002). High performance functionally graded and segmented Bi_2Te^3-based materials for thermoelectric power generation. *Journal of Materials Science*. 37(14), 2893-2897. https://doi.org/10.1023/A:1016092224833.

[10] Yan, X., Tang, N., LIU, X., SHUI, G., Xu, Q., & Liu, B. (2015). Modeling and simulation of directional solidification by LMC process for nickel base superalloy casting. *Acta Metallurgica Sinica*. 51(10), 1288-1296. DOI: 10.11900/0412.1961.2015.00338.